RESEARCH ARTICLE
doi: 10.2306/scienceasia1513-1874.2025.083

ScienceAsia 51 (5): 2025: ID 2025083: **1–8**

Tangeretin protects mice from sepsis-induced myocardial injury by inhibiting TRIM8 expression through upregulation of miR-20a-5p

Ji Shi, QiYin Sun*

Department of Cardiology, Huzhou First People's Hospital, Zhejiang 313000 China

*Corresponding author, e-mail: dr.sunqiyin@outlook.com

Received 10 Oct 2024, Accepted 15 Sep 2025
Available online 31 Oct 2025

ABSTRACT: In this study, tangeretin (TAN), a plant-derived flavonoid, was investigated for its role in sepsis-induced myocardial injury (SIMI). C57BL/6 mice were gavaged daily with 50 mg/kg TAN, while lentiviruses interfering with miR-20a-5p or TRIM8 expression were injected into the tail vein for three consecutive days. Then, a mouse model of sepsis was established by cecum ligation puncture (CLP). Levels of serum myocardial injury markers (CK-MB and cTnI) were detected by a fully automated analyzer. The histopathology of mouse myocardium was observed by HE staining. Apoptosis was detected by TUNEL staining in mouse myocardial tissues. TAN improved cardiac dysfunction and myocardial injury in CLP mice. TAN could upregulate miR-20a-5p and downregulate TRIM8 levels. The beneficial effects of TAN could be attenuated by downregulating miR-20a-5p or upregulating TRIM8. TAN protects mice from SIMI by inhibiting TRIM8 expression through upregulation of miR-20a-5p.

KEYWORDS: tangeretin, miR-20a-5p, TRIM8, sepsis, myocardial injury

INTRODUCTION

Sepsis, a prevalent critical condition in clinical settings [1], is a systemic inflammatory response syndrome caused by excessive secretion of endotoxin lipopolysaccharide (LPS) due to microbial infection in the blood. Septic shock can cause multiple organ failure until death if no effective treatments are available [2, 3]. Recently, attention has focused on the harmful effects of endotoxin on the heart. Sepsis, as reported, causes myocardial injury and cardiac dysfunction that can lead to marked mortality [4, 5]. Since sepsis-induced myocardial injury (SIMI) is highly fatal and there are no safe and effective treatments available [6], a key aspect of the study of SIMI is discovering the pathogenesis and looking for effective prevention and treatment methods.

Tangeretin (TAN) is a flavonoid found primarily in citrus fruits, which exhibits anti-inflammatory and antioxidant properties [7, 8]. TAN is protective against SIMI by inhibiting the PTEN/AKT/mTOR axis [9]. In septic mice, TAN inhibits ROS-mediated NLRP3 inflammasome activation by regulating PLK1/AMPK/DRP1 signaling [10]. However, the specific regulatory mechanisms of TAN in SIMI have not been fully investigated.

Non-coding RNAs (ncRNAs), including circular RNAs, long-stranded non-coding RNAs, and microRNAs (miRNAs), are key components of the cellular gene expression regulatory network [11–13]. Almost all major cellular functions, including proliferation and apoptosis, are regulated by miRNAs [14], and miRNAs also contribute to diseases such as sepsis and heart disease [15–18]. MiRNA dysregulation during sepsis exacerbates sepsis-associated disorders [19–22]. In this way, studying the biological role and molecular mechanisms of miRNA in SIMI is useful for identifying new therapeutic targets.

Increasing miR-20a-5p expression prevents diabetic cardiomyopathy by inhibiting cardiomyocyte hypertrophy, apoptosis, and fibrosis [23]. By regulating the E2F1/p73 signaling pathway, miR-20a-5p targets E2F1 and inhibits cardiomyocyte apoptosis [24]. Despite this, there is no clear association between miR-20a-5p and SIMI. This study therefore investigated the role and mechanism of TAN in SIMI by upregulating miR-20a-5p.

MATERIALS AND METHODS

Animals

Eight-week-old male C57BL/6 mice (25–30 g, Shanghai Southern Model Biotechnology, China) were housed in a light/dark cycle and temperature-controlled environment for 12 h under standardized laboratory conditions. The mice were raised in cages (4–5 mice/cage) at 22 ± 1 °C with 50 ± 5% humidity. Each cage was supplied with food and water. Animal experiments were approved by the Animal Care Committee of Huzhou First People's Hospital (No. 202209HZ263).

Sepsis modeling

As previously described, sepsis was established by cecal ligation and puncture (CLP) [25]. After anesthesia using an intraperitoneal injection of pentobarbital sodium (30 mg/kg), the cecum was exposed through a 1–2 cm midline incision across the abdomen. Immediately below the ileocecal valve, the cecum was ligated

with a 5–0 silk thread. Two punctures were made with an 18-gauge needle from the point of ligation to the tip of the cecum, and a drainage tube was attached. The cecum was gently squeezed to drain the feces and relocated to the abdomen. Each mouse was injected with warm saline (0.05 ml/g).

Animal grouping

Mice were randomly divided into 9 groups (6 mice in each group): 1) Sham group; 2) Model group; 3) TAN group; 4) TAN + lentiviral vector (LV)-negative control (NC) group; 5) TAN + LV-miR-20a-5p group; 6) TAN + LV-anti-NC group; 7) TAN + LV-anti-miR-20a-5p group; 8) TAN + LV-overexpression (oe)-NC group; 9) TAN + LV-oe-TRIM8 group. The specific treatments for each group of mice are shown in Table S1. TAN was purchased from Sigma-Aldrich (Shanghai, China). Lentiviral vectors carrying cardiac Troponin I (cTnI) promoter were generated by Hanbio Biotechnology (Shanghai, China).

Cardiac function

Twenty-four hours after CLP treatment, mice were given an intraperitoneal injection of pentobarbital sodium (30 mg/kg), immobilized on a thermostatic detector plate, and subjected to echocardiography using a VisualSonics Vevo 770 system and a 30 MHz ultrasound probe. Left ventricular internal diameter at end-diastole (LVIDd), left ventricular internal diameter at end-systole (LVIDs), and left ventricular ejection fraction (EF) were measured.

Biochemical analysis

Following the echocardiography, the mice were euthanized with an intraperitoneal injection of pentobarbital sodium at a dose of 100 mg/kg, and 500 μl of blood was collected. Counts of platelets (PLT) and white blood cells (WBC) were measured using an ABX Micros 60 Hematology Analyzer (Horiba-ABX, Montpellier, France). The collected blood was allowed to stand at 4 °C for 8 h. After centrifugation at 3000 r/min for 15 min, the supernatant was collected as serum. Tumor necrosis factor-α (TNF-α), interleukin (IL)-6, and IL-1β in serum were measured using enzyme-linked immunosorbent assay (ELISA) kits (R&D Systems, MN, USA). Meanwhile, creatine kinase-MB (CK-MB) and cTnI in serum were measured using the corresponding kits (Nanjing Jiancheng, Nanjing, China). Serum aspartate aminotransferase (AST) and alanine aminotransferase (ALT) levels were detected using a Beckman automatic biochemical analyzer (Roche, Germany). Serum creatinine (Scr) and blood urea nitrogen (BUN) were measured utilizing a colorimetric method and a creatinine assay kit (Nanjing Jiancheng).

Sample collection

The left ventricle of the mouse heart was isolated and cut into three parts along the short axis, perpendicular to its long axis. The apical part was fixed by 4% paraformaldehyde for histopathological staining, the middle part was snap-frozen in liquid nitrogen for total RNA extraction, and the base was snap-frozen in liquid nitrogen for protein extraction.

HE staining

After being fixed in 4% paraformaldehyde for 24 h, the apical section of the left ventricle was dehydrated, cleared, and embedded in paraffin. Sections from the specimens were cut using a microtome and stained with HE for 5 min. Microscope images were taken under a light microscope (Olympus, Tokyo, Japan).

TUNEL staining

TUNEL staining was performed in myocardial tissues using the In Situ Cell Death Detection Kit (Roche, Mannheim, Germany). Apoptosis index was calculated as the percentage of TUNEL-positive cells (brown) under a light microscope (Olympus).

RT-qPCR

Total RNA from mid-ventricle was extracted using TRIzol reagent (Takara, Tokyo, Japan). RNA was reverse transcribed into cDNA using the Prime Script RT reagent Kit (Takara). ABI 7900HT RT-PCR system settings (Thermo Fisher Scientific, Waltham, USA) were used with SYBR® Premix Ex TaqTM II (Takara) for RT-qPCR. Amplification was initiated at 95 °C for 10 s, followed by 40 cycles of 95 °C for 5 s, 60 °C for 31 s, and 72 °C for 15 s. miR-20a-5p and TRIM8 levels were quantified using the $2^{-\Delta\Delta CT}$ method and normalized to U6 or GAPDH. Primers were synthesized by Sangon (Shanghai, China), as shown in Table S2.

Western blot analysis

The basal base of the mouse left ventricle (approximately 50 mg) was taken, ground in liquid nitrogen, added to 500 μl of RIPA lysis buffer (containing protease/phosphatase inhibitors), and lysed on ice for 30 min. Centrifugation was performed for 15 min at 14,000 × *g* at 4 °C, and the supernatant was collected. Protein concentration was determined using the BCA method. Using 10% SDS-PAGE, equal amounts of protein were separated and transferred to a PVDF membrane (Millipore, Burlington, USA), which was blocked with 5% skim milk for 1 h. Incubation with primary antibodies against TRIM8 (1:1000, Abcam, Shanghai, China) and GAPDH (1:1000, Abcam) was carried out overnight at 4 °C on PVDF membranes, followed by peroxidase-conjugated goat anti-rabbit IgG secondary antibody at room temperature for 2 h. Blots were quantified with ImageJ software based on ECL reagent (Advansta, CA, USA).

Luciferase reporter assay

The miR-20a-5p and TRIM8 targeting binding sites were predicted using the bioinformatics website star-

Base (https://starbase.sysu.edu.cn/). The corresponding sequences were inserted into the luciferase reporter vector pmirGLO (Promega, Madison, USA), and TRIM8-WT and TRIM8-MUT were constructed. The constructed vectors were co-transfected with miR-20a-5p mimic or mimic NC into HEK293T cells (BeNa Culture Collection, Shanghai, China), cells were collected and lysed 48 h after transfection, and luciferase activities were detected using a dual luciferase assay system (Promega).

Statistical analysis

Data were analyzed using SPSS 22.0 (IBM, NY, USA). Data were presented as mean ± standard deviation (SD). Independent two-sample *t*-tests were used for comparisons between two groups, while one-way analysis of variance (ANOVA) followed by Tukey's post hoc test was applied for comparisons among multiple groups. Statistical significance was defined as $p < 0.05$, with each experiment conducted with at least three biological replicates.

RESULTS

Amelioration of cardiac dysfunction and myocardial injury by TAN in CLP mice

A sepsis mouse model was established by CLP. PLT counts and leukocyte counts were performed using ABX Micros 60 Hematology Analyzer, and levels of serum inflammatory factors (TNF-α, IL-1β and IL-6) were determined by ELISA. PLT counts were decreased, leukocyte counts were elevated (Fig. S1A,B), and serum inflammatory factors (TNF-α, IL -1β, and IL-6) were increased (Fig. S1C–E), indicating successful establishment of the sepsis mouse model. After gavage administration of TAN to normal mice for 3 consecutive days, no significant changes in serum biomarkers for liver, renal, and cardiac functions were observed (Fig. S2A–F), suggesting that 50 mg/kg of TAN has low toxicity. Three days before CLP, mice were gavaged with 50 mg/kg TAN daily. LVIDd, LVIDs, and EF were decreased in CLP mice, indicating that cardiac dysfunction was present in CLP mice, whereas TAN markedly improved the cardiac function in CLP mice (Fig. 1A,B). Serum CK-MB and cTnI levels were increased in CLP mice, while TAN significantly decreased CK-MB and cTnI levels (Fig. 1C,D). Myocardial histopathology was observed by HE staining, which showed that CLP mice had focal degenerative necrosis of cardiomyocytes and inflammatory cell infiltration, whereas TAN significantly improved myocardial histopathology (Fig. 1E). Detection of apoptosis in myocardial tissues by TUNEL staining showed that apoptosis was increased in myocardial tissues of CLP mice, whereas TAN significantly reduced apoptosis in myocardial tissues (Fig. 1F).

Forcing miR-20a-5p expression enhancing the ameliorative effect of TAN on cardiac dysfunction and myocardial injury in CLP mice

Detection of miR-20a-5p expression by RT-qPCR showed that miR-20a-5p expression was reduced in CLP mice, whereas TAN could promote miR-20a-5p expression (Fig. 2A). Mice were gavaged with 50 mg/kg TAN daily, while mimic NC or miR-20a-5p mimic lentivirus was injected into the tail vein, and the success of the lentivirus injection was verified by RT-qPCR (Fig. 2B). It was shown that enhancing miR-20a-5p further improved cardiac dysfunction and myocardial injury in CLP mice (Fig. 2C–H).

Reducing miR-20a-5p weakening the ameliorative effects of TAN on CLP mice

Mice were gavaged with 50 mg/kg TAN daily and simultaneously injected with inhibitor NC or miR-20a-5p inhibitor lentivirus via the tail vein, and the success of lentiviral injection was verified by RT-qPCR (Fig. 3A). The experimental analysis supported that lowering miR-20a-5p attenuated the ameliorative effects of TAN on cardiac dysfunction and myocardial injury in CLP mice (Fig. 3B–G).

TRIM8 targeted by miR-20a-5p

To further investigate how miR-20a-5p affects the therapeutic efficacy of TAN in SIMI, we explored the direct target genes of miR-20a-5p. TRIM8 had a binding site for miR-20a-5p (Fig. 4A). Dual luciferase reporter assay also confirmed that miR-20a-5p could bind to TRIM8 (Fig. 4B). Interestingly, TAN could inhibit TRIM8 mRNA and protein expression (Fig. 4C,D). To further determine whether the TAN-induced elevation of TRIM8 expression was mediated by miR-20a-5p, we examined TRIM8 mRNA and protein expression by RT-qPCR and Western blot analysis, which showed that upregulating miR-20a-5p further enhanced the downregulating effect of TAN on TRIM8 mRNA and protein expression, while downregulating miR-20a-5p attenuated this effect (Fig. 4E,F). In addition, we also found that upregulation of miR-20a-5p inhibited TRIM8 expression and downregulation of miR-20a-5p promoted TRIM8 expression (Fig. S3A,B). These results suggest that TRIM8 is a direct target gene of miR-20a-5p and that TAN inhibits TRIM8 expression by upregulating miR-20a-5p.

Upregulation of TRIM8 attenuating TAN's ameliorative effects on cardiac dysfunction and myocardial injury in CLP mice

To elucidate whether TRIM8 mediated the effect of TAN in SIMI, mice were gavaged with 50 mg/kg TAN daily for 3 days before CLP, while oe-NC or oe-TRIM8 lentiviruses were injected into the tail vein, and the success of the lentiviral injections was verified by RT-qPCR and Western blot analysis (Fig. 5A,B). The exper-

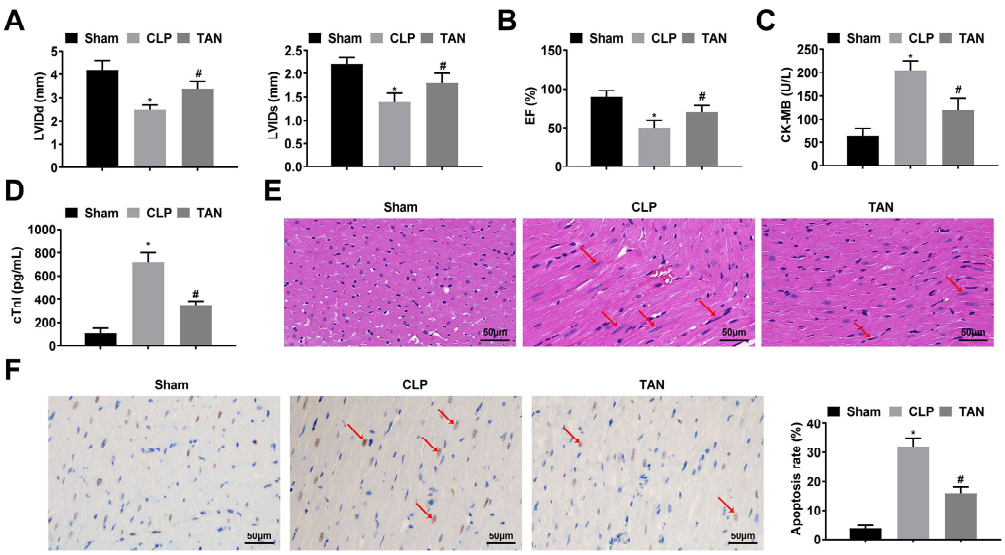

Fig. 1 TAN improving cardiac dysfunction and myocardial injury in CLP mice. A/B: Echocardiography to detect cardiac function in mice; C/D: Serum CK-MB and cTnI levels; E: HE staining to observe the pathology of myocardial tissue in mice (Arrows indicate necrotic cells); F: TUNEL staining to detect apoptosis in myocardial tissue in mice (Arrows indicate apoptotic cells). Values are expressed as mean ± SD. Comparisons between two groups were made using independent samples *t*-test while comparisons between multiple groups used one-way ANOVA and Tukey's post hoc test. * indicates $p < 0.05$ compared with Sham group; # indicates $p < 0.05$ compared with CLP group.

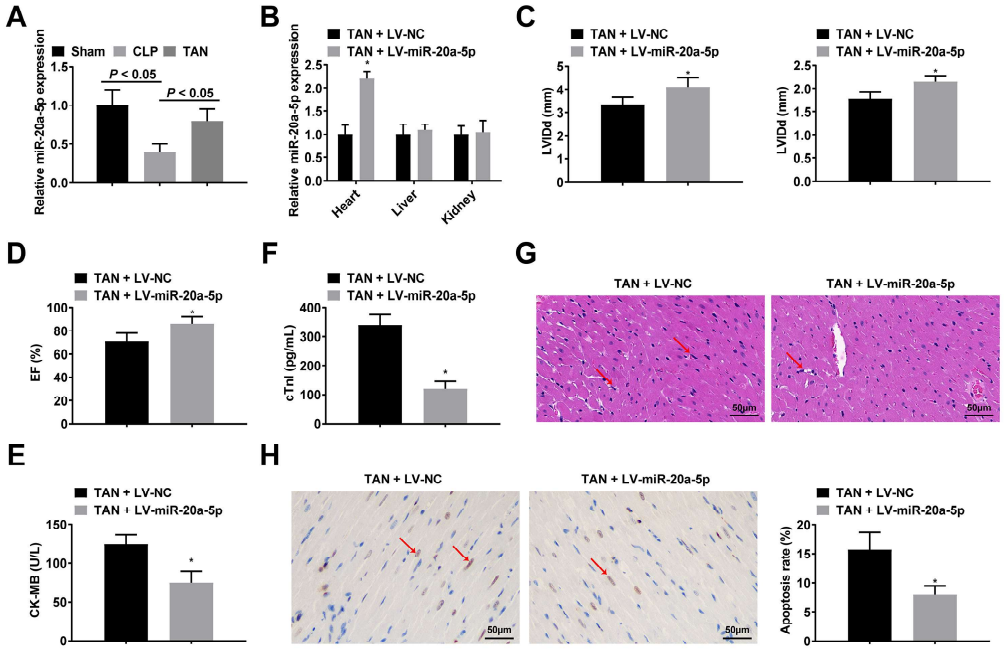

Fig. 2 Upregulation of miR-20a-5p enhancing the ameliorative effect of TAN on cardiac dysfunction and myocardial injury in CLP mice. A/B: RT-qPCR to detect miR-20a-5p expression; C/D: Echocardiography to detect cardiac function in mice; E/F: Serum CK-MB and cTnI levels; G: HE staining to observe the pathology of myocardial tissue in mice (Arrows indicate necrotic cells); H: TUNEL staining to detect apoptosis in myocardial tissue in mice (Arrows indicate apoptotic cells). Values are expressed as mean ± SD. Comparisons between two groups were made using independent samples *t*-test while comparisons between multiple groups used one-way ANOVA and Tukey's post hoc test. * indicates $p < 0.05$ compared with Sham group; # indicates $p < 0.05$ compared with CLP group; & indicates $p < 0.05$ compared with TAN + LV-NC group.

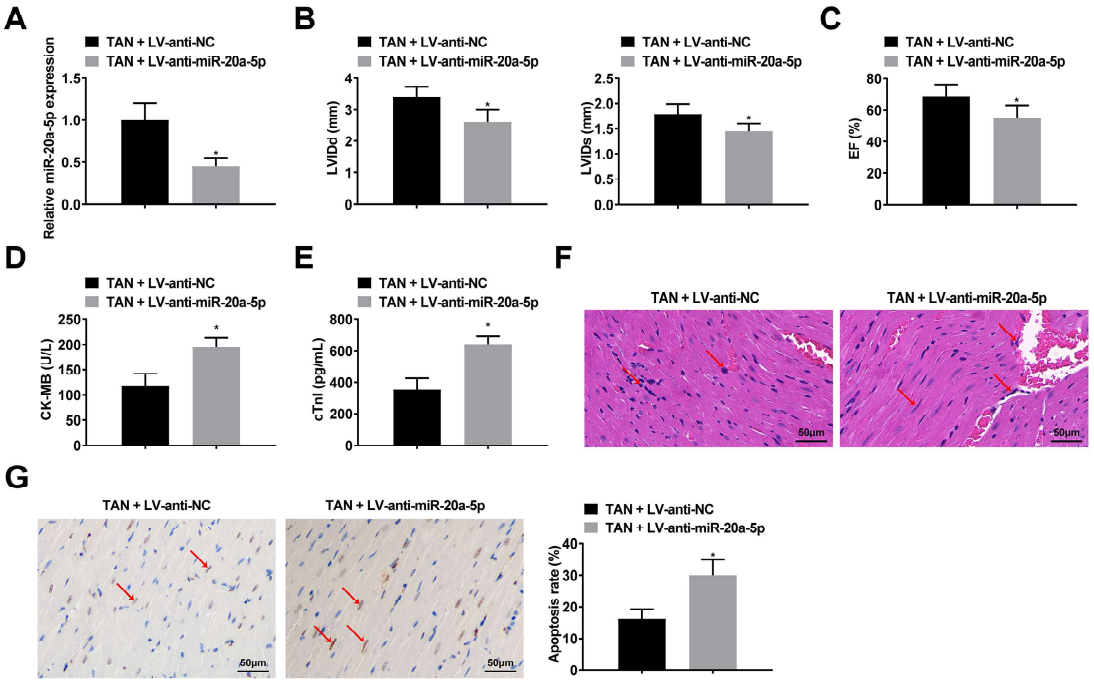

Fig. 3 Downregulation of miR-20a-5p attenuating the ameliorative effect of TAN on cardiac dysfunction and myocardial injury in CLP mice. A: RT-qPCR to detect miR-20a-5p expression; B/C: Echocardiography to detect cardiac function in mice; D/E: Serum CK-MB and cTnI levels; F: HE staining to observe the pathology of myocardial tissues in mice (Arrows indicate necrotic cells); G: TUNEL staining to detect apoptosis in myocardial tissues of mice (Arrows indicate apoptotic cells). Values are expressed as mean ± SD. Comparisons between two groups were made using independent samples *t*-test while comparisons between multiple groups used one-way ANOVA and Tukey's post hoc test. * indicates $p < 0.05$ compared with TAN + LV-anti-NC group.

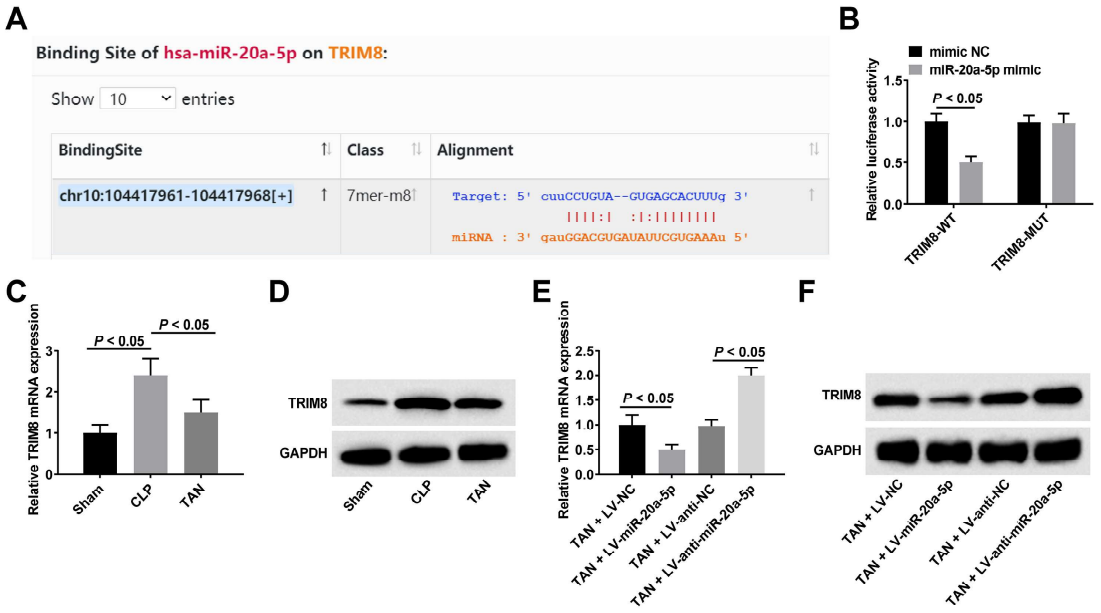

Fig. 4 TRIM8 as a direct target gene of miR-20a-5p. A: Prediction of the binding site of miR-20a-5p and TRIM8 by bioinformatics website starBase; B: Confirmation of miR-20a-5p binding to TRIM8 by dual luciferase reporter assay; C–F: RT-qPCR and Western blot analysis of TRIM8 expression. Values are expressed as mean ± SD. Comparisons between two groups were made using independent samples *t*-test while comparisons between multiple groups used one-way ANOVA and Tukey's post hoc test.

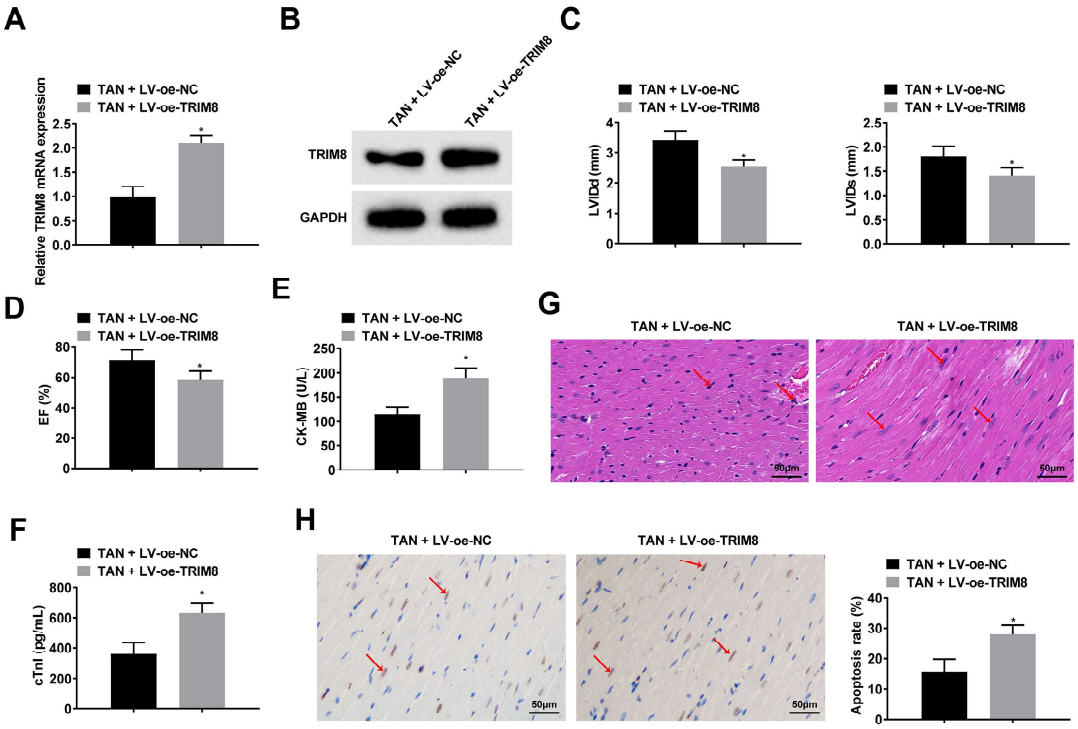

Fig. 5 Upregulation of TRIM8 reversing the ameliorative effect of TAN on cardiac dysfunction and myocardial injury in CLP mice. A/B: RT-qPCR and Western blot analysis to detect TRIM8 expression; C/D: Echocardiography to detect cardiac function in mice; E/F: Serum CK-MB and cTnI levels; G: HE staining to observe the pathology of myocardial tissues in mice (Arrows indicate necrotic cells); H: TUNEL staining to detect apoptosis in myocardial tissues in mice (Arrows indicate apoptotic cells). Values are expressed as mean ± SD. Comparisons between two groups were made using independent samples t-test while comparisons between multiple groups used one-way ANOVA and Tukey's post hoc test. * indicates $p < 0.05$ compared with TAN + LV-oe-NC group.

imental results showed that upregulating TRIM8 attenuated TAN's ameliorative effects on cardiac dysfunction and myocardial injury (Fig. 5C–H).

DISCUSSION

The CLP technique was utilized in this study to induce sepsis in mice. This technique is frequently employed for *in vivo* sepsis modeling [26]. A puncture in the cecum, which is rich in bacteria, causes polymicrobial peritonitis, allowing bacteria to translocate into the blood, leading to bacteremia, septic shock, multi-organ dysfunction, and ultimately death [27]. CLP is widely regarded as a more accurate representation of clinical reality compared to earlier methods like injecting endotoxin or purified bacteria into rodents. Therefore, CLP is considered the benchmark (though it has its limitations) for experimental induction [28]. Severe sepsis and septic shock are major medical problems in critical patients infected with pathogenic microorganisms [29, 30]. Heart damage caused by sepsis has serious adverse effects on patients, and the severity of myocardial damage determines patient outcomes [31]. EF and cardiac output are reduced as a result of SIMI, which increases mortality risk substantially [32]. CLP-induced sepsis produced myocardial injury evident in the form of vasodilatation and congestion, focal degeneration, cardiomyocyte necrosis/apoptosis, as well as inflammatory cell infiltration. CLP mice also had severely impaired cardiac function, with significantly decreased LVIDd, LVIDs, and EF. Myocardial histopathology was improved in CLP mice treated with TAN, and LVIDd, LVIDs, and EF were elevated. As an indicator of left ventricular systolic function, EF reflects the shortening of left ventricular fibers [33]. CLP mice with significant increases in EF show that TAN can relieve cardiac dysfunction.

In this study, miR-20a-5p expression was reduced in CLP mice, whereas TAN could promote miR-20a-5p expression. In addition, upregulating miR-20a-5p enhanced the ameliorative effects of TAN on cardiac dysfunction and myocardial injury in CLP mice, whereas downregulating miR-20a-5p attenuated this effect. These results suggest that TAN ameliorates cardiac dysfunction and myocardial injury in CLP mice by upregulating miR-20a-5p.

Gene expression is negatively regulated by miRNAs, which inhibit or degrade target mRNAs by interacting with their 3′ untranslated regions [34]. TRIM8

was determined to be a downstream target of miR-20a-5p using bioinformatics analysis of the miR-20a-5p transcript. Multiple pathological processes, such as inflammation, cancer, and immune responses, are regulated by TRIM8 [35, 36]. A pro-inflammatory effect of TRIM8 is observed in *Pseudomonas aeruginosa*-induced keratitis [37]. In hepatic ischemia/reperfusion injury models, TRIM8 is also upregulated, which can aggravate the injury by activating the TAK1-dependent pathway [38]. LPS-induced acute lung injury is alleviated by silencing TRIM8 due to its significant anti-inflammatory and antioxidant effects [39]. It is evident from these studies that TRIM8 exacerbates sepsis by promoting inflammation. In this study, TRIM8 expression was upregulated in CLP mice, and TAN inhibited TRIM8 expression. Upregulating miR-20a-5p inhibited TRIM8 expression, and downregulating miR-20a-5p promoted TRIM8 expression. Upregulation of TRIM8 reversed the beneficial effects of TAN on cardiac dysfunction and myocardial injury in CLP mice. Therefore, we hypothesized that TAN protects mice from SIMI by inhibiting TRIM8 expression through upregulation of miR-20a-5p.

However, this study still has some limitations. First, this study only investigated the therapeutic effect of 50 mg/kg TAN in CLP mice, and more experiments are needed to clarify the optimal effective concentration of TAN. Second, this study did not investigate the long-term protective effect of TAN and the therapeutic value of post-CLP interventions, and the time-dependent effects of TAN should be further characterized in subsequent studies, especially to validate the therapeutic potential of TAN after the onset of cardiac injury. Furthermore, this study only focused on the role of miR-20a-5p and TRIM8 in sepsis, whereas TAN may regulate other pathways in CLP. The study was limited to examining the roles of miR-20a-5p and TRIM8 in sepsis, but TAN could potentially influence CLP mice therapeutically via different pathways, indicating a need for further investigation.

CONCLUSION

TAN can protect mice from SIMI by inhibiting TRIM8 expression through upregulating miR-20a-5p. TAN appears to be a potential candidate for treating SIMI.

Appendix A. Supplementary data

Supplementary data associated with this article can be found at https://dx.doi.org/10.2306/scienceasia1513-1874.2025.083.

REFERENCES

1. Angus DC, Pereira CA, Silva E (2006) Epidemiology of severe sepsis around the world. *Endocr Metab Immune Disord Drug Targets* **6**, 207–212.
2. Maloney, PJ (2013) Sepsis and septic shock. *Emerg Med Clin North Am* **31**, 583–600.
3. Singer M, Deutschman CS, Seymour CW, Shankar-Hari M, Annane D, Bauer M, Bellomo R, Bernard GR, et al (2016) The third international consensus definitions for sepsis and septic shock (Sepsis-3). *JAMA* **315**, 801–810.
4. Chen J, Wang B, Lai J, Braunstein Z, He M, Ruan G, Yin Z, Wang J, et al (2018). Trimetazidine attenuates cardiac dysfunction in endotoxemia and sepsis by promoting neutrophil migration. *Front Immunol* **9**, 2015.
5. Hunter JD, Doddi M (2010) Sepsis and the heart. *Br J Anaesth* **104**, 3–11.
6. Venkataraman R, Subramanian S, Kellum JA (2003) Clinical review: Extracorporeal blood purification in severe sepsis. *Crit Care* **7**, 139–145.
7. Sedik AA, Elgohary R (2023) Neuroprotective effect of tangeretin against chromium-induced acute brain injury in rats: targeting Nrf2 signaling pathway, inflammatory mediators, and apoptosis. *Inflammopharmacology* **31**, 1465–1480.
8. Xin X, Yao D, Zhang K, Han S, Liu D, Wang H, Liu X, Li G, et al (2019) Protective effects of Rosavin on bleomycin-induced pulmonary fibrosis via suppressing fibrotic and inflammatory signaling pathways in mice. *Biomed Pharmacother* **115**, 108870.
9. Shiroorkar PN, Afzal O, Kazmi I, Al-Abbasi FA, Altamimi ASA, Gubbiyappa KS, Sreeharsha N (2020) Cardioprotective effect of tangeretin by inhibiting PTEN/AKT/m-TOR axis in experimental sepsis-induced myocardial dysfunction. *Molecules* **25**.
10. Liu Y, Zhang Y, You G, Zheng D, He Z, Guo W, Antonina K, Shukhrat Z, et al (2024) Tangeretin attenuates acute lung injury in septic mice by inhibiting ROS-mediated NLRP3 inflammasome activation via regulating PLK1/AMPK/DRP1 signaling axis. *Inflamm Res* **73**, 47–63.
11. Patop IL, Wust S, Kadener S (2019) Past, present, and future of circRNAs. *Embo J* **38**, e100836.
12. Pu J, Zhao Y, Bai X, Feng T, Lu W, Ding L, Yu Q (2024) Cyclic intermittent hypoxia induces apoptosis through upregulation of LncRNA GAS5 expression in cardiomyocyte. *ScienceAsia* **50**, ID 2024061.
13. Li J, Zhu Z, Ren Z, Li G (2023) Silencing circRNA TLK1 reduces endothelial cell injury in coronary heart disease. *ScienceAsia* **49**, 899–909.
14. Zhelankin AV, Vasiliev SV, Stonogina DA, Babalyan KA, Sharova EI, Doludin YV, Shchekochikhin DY, Generozov EV, et al (2020) Elevated plasma levels of circulating extracellular miR-320a-3p in patients with paroxysmal atrial fibrillation. *Int J Mol Sci* **21**.
15. Halushka PV, Goodwin AJ, Halushka MK (2019) Opportunities for microRNAs in the crowded field of cardiovascular biomarkers. *Annu Rev Pathol* **14**, 211–238.
16. Wang L, Wang HC, Chen C, Zeng J, Wang Q, Zheng L, Yu HD (2013) Differential expression of plasma miR-146a in sepsis patients compared with non-sepsis-SIRS patients. *Exp Ther Med* **5**, 1101–1104.
17. Wang X, Zhang X, Ren XP, Chen J, Liu H, Yang J, Medvedovic M, Hu Z, et al (2010) MicroRNA-494 targeting both proapoptotic and antiapoptotic proteins protects against ischemia/reperfusion-induced cardiac injury. *Circulation* **122**, 1308–1318.
18. Yu Y, Gao R, Kaul Z, Li L, Kato Y, Zhang Z, Groden J, Kaul SC, et al (2016) Loss-of-function screening to identify miRNAs involved in senescence: tumor suppressor activity of miRNA-335 and its new target CARF. *Sci Rep* **6**, 30185.

19. Ge C, Liu J, Dong S (2018) miRNA-214 Protects sepsis-induced myocardial injury. *Shock* **50**, 112–118.
20. Tacke F, Roderburg C, Benz F, Cardenas DV, Luedde M, Hippe HJ, Frey N, Vucur M, et al (2014) Levels of circulating miR-133a are elevated in sepsis and predict mortality in critically ill patients. *Crit Care Med* **42**, 1096–1104.
21. Wang H, Meng K, Chen W, Feng D, Jia Y, Xie L (2012) Serum miR-574-5p: a prognostic predictor of sepsis patients. *Shock* **37**, 263–267.
22. Wang HJ, Zhang PJ, Chen WJ, Feng D, Jia YH, Xie LX (2012) Four serum microRNAs identified as diagnostic biomarkers of sepsis. *J Trauma Acute Care Surg* **73**, 850–854.
23. Liu X, Guo B, Zhang W, Ma B, Li Y (2021) MiR-20a-5p overexpression prevented diabetic cardiomyopathy via inhibition of cardiomyocyte apoptosis, hypertrophy, fibrosis and JNK/NF-κB signalling pathway. *J Biochem* **170**, 349–362.
24. Wang Y, Chen L, Wang L, Pei G, Cheng H, Zhang Q, Wang S, Hu D, et al (2023) Pulsed electromagnetic fields combined with adipose-derived stem cells protect ischemic myocardium by regulating miR-20a-5p/E2F1/p73 signaling. *Stem Cells* **41**, 724–737.
25. Haak BW, Prescott HC, Wiersinga WJ (2018) Therapeutic potential of the gut microbiota in the prevention and treatment of sepsis. *Front Immunol* **9**, 2042.
26. Li JL, Li G, Jing XZ, Li YF, Ye QY, Jia HH, et al (2018) Assessment of clinical sepsis-associated biomarkers in a septic mouse model. *J Int Med Res* **46**, 2410–2422.
27. Deitch EA (2005) Rodent models of intra-abdominal infection. *Shock* **24**(S1), 19–23.
28. Raven K (2012) Rodent models of sepsis found shockingly lacking. *Nat Med* **18**, 998.
29. Rello J, Valenzuela-Sanchez F, Ruiz-Rodriguez M, Moyano S (2017) Sepsis: A review of advances in management. *Adv Ther* **34**, 2393–2411.
30. Wang X, Yu Y (2018) MiR-146b protect against sepsis induced mice myocardial injury through inhibition of Notch1. *J Mol Histol* **49**, 411–417.
31. Ehrman RR, Sullivan AN, Favot MJ, Sherwin RL, Reynolds CA, Abidov A, et al (2018) Pathophysiology, echocardiographic evaluation, biomarker findings, and prognostic implications of septic cardiomyopathy: A review of the literature. *Crit Care* **22**, 112.
32. Fattahi F, Ward PA (2017) Complement and sepsis-induced heart dysfunction. *Mol Immunol* **84**, 57–64.
33. Yan F, Wang Q, Yang H, Lv H, Qin W (2023) miR-926-3p influences myocardial injury in septic mice through regulation of mTOR signaling pathway by targeting TSC1. *Aging (Albany NY)* **15**, 3826–3838.
34. Meng S, Zhou H, Feng Z, Xu Z, Tang Y, Li P, et al (2017) CircRNA: functions and properties of a novel potential biomarker for cancer. *Mol Cancer* **16**, 94.
35. Mastropasqua F, Marzano F, Valletti A, Aiello I, Di Tullio G, Morgano A, et al (2017) TRIM8 restores p53 tumour suppressor function by blunting N-MYC activity in chemo-resistant tumours. *Mol Cancer* **16**, 67.
36. Ye W, Hu MM, Lei CQ, Zhou Q, Lin H, Sun MS, et al (2017) TRIM8 negatively regulates TLR3/4-mediated innate immune response by blocking TRIF-TBK1 interaction. *J Immunol* **199**, 1856–1864.
37. Guo L, Dong W, Fu X, Lin J, Dong Z, Tan X, et al (2017) Tripartite motif 8 (TRIM8) positively regulates pro-inflammatory responses in *Pseudomonas aeruginosa*-induced keratitis through promoting K63-linked polyubiquitination of TAK1 protein. *Inflammation* **40**, 454–463.
38. Tao Q, Tianyu W, Jiangqiao Z, Zhongbao C, Xiaoxiong M, Long Z, et al (2019) Tripartite motif 8 deficiency relieves hepatic ischaemia/reperfusion injury via TAK1-dependent signalling pathways. *Int J Biol Sci* **15**, 1618–1629.
39. Xiaoli L, Wujun Z, Jing L (2019) Blocking of tripartite motif 8 protects against lipopolysaccharide (LPS)-induced acute lung injury by regulating AMPKα activity. *Biochem Biophys Res Commun* **508**, 701–708.

Appendix A. Supplementary data

Table S1 Grouping and treatment of animals.

Group	Treatment
Sham	Cecum exposure only without CLP
Model	CLP treatment
TAN	3 days prior to CLP, 50 mg/kg TAN by gavage daily
TAN + LV-NC	3 days prior to CLP, 50 mg/kg TAN by gavage and 5×10^7 TU LV-NC by tail vein daily
TAN + LV-miR-1226-3p	3 days prior to CLP, 50 mg/kg TAN by gavage and 5×10^7 TU LV-miR-1226-3p by tail vein injection
TAN + LV-anti-NC	3 days prior to CLP, 50 mg/kg TAN by gavage and 5×10^7 TU LV-anti-NC by tail vein daily
TAN + LV-anti-miR-1226-3p	3 days prior to CLP, 50 mg/kg TAN by gavage and 5×10^7 TU LV-anti-miR-1226-3p by tail vein daily
TAN + LV-oe-NC	3 days prior to CLP, 50 mg/kg TAN by gavage and 5×10^7 TU LV-oe-NC by tail vein daily
TAN + LV-oe-TRIM8	3 days prior to CLP, 50 mg/kg TAN by gavage and 5×10^7 TU LV-oe-TRIM8 by tail vein daily

CLP, cecum ligation puncture; Tan, tangeretin; LV, lentiviral vector; NC, negative control; oe, overexpression.

Table S2 RT-qPCR primers.

Gene	Sequence (5′–3′)
miR-20a-5p	Forward: AGGGCTAAAGTGCTTATAGTGC Reverse: TCCTCCTCTCCTCTCCTCTC
TRIM8	Forward: GTGGAGATACGGAGGAATGAGA Reverse: TGGTGCAGCTTTTCGTACTGC
U6	Forward: CTCGCTTCGGCAGCACA Reverse: AACGCTTCACGAATTTGCGT
GAPDH	Forward: CACCCACTCCTCCACCTTTG Reverse: CCACCACCCTGTTGCTGTAG

TRIM8, TRIB3 recruits tripartite motif containing 8; GAPDH, glyceraldehyde 3-phosphate dehydrogenase.

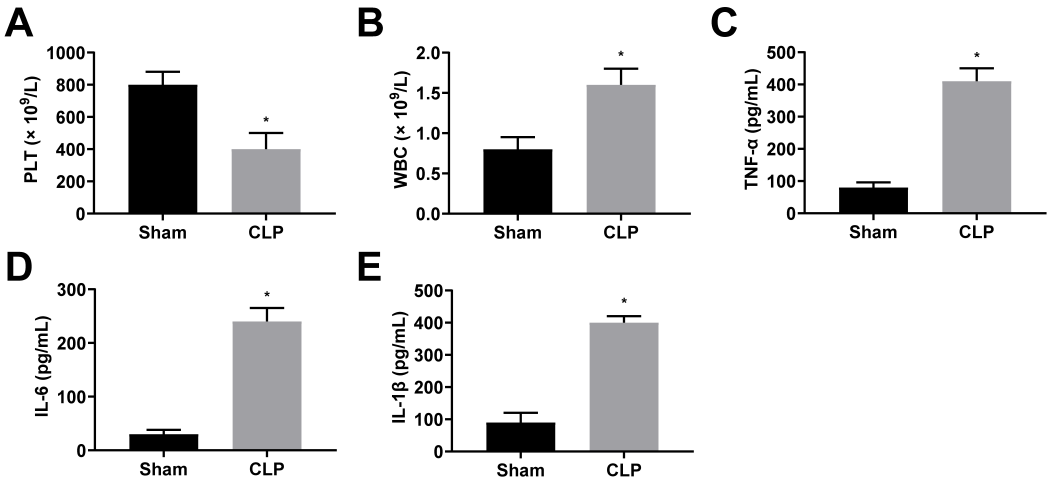

Fig. S1 Successful establishment of a mouse model of sepsis. A/B: ABX Micros 60 Hematology Analyzer for PLT count and WBC count; C–E: ELISA for serum levels of inflammatory factors (TNF-α, IL-1β and IL-6). Values are expressed as mean ± SD. Comparisons between two groups were made using independent samples *t*-test while comparisons between multiple groups used one-way ANOVA and Tukey's post hoc test. * indicates $p < 0.05$ compared with Sham group; # indicates $p < 0.05$ compared with CLP group.

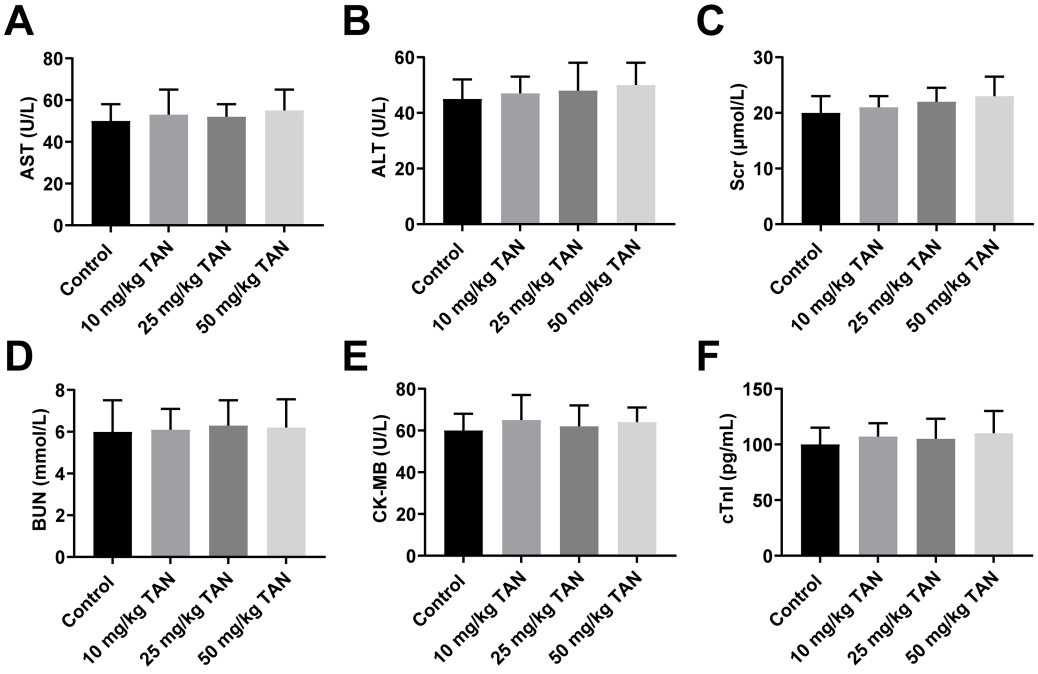

Fig. S2 TAN exhibiting low toxicity. A/B: Levels of liver function biomarkers (AST and ALT); C/D: Levels of kidney function biomarkers (Scr and BUN); E/F: Levels of cardiac function biomarkers (CK-MB and cTnI). Values are expressed as mean ± SD. Comparisons between two groups were made using independent samples *t*-test while comparisons between multiple groups used one-way ANOVA and Tukey's post hoc test.

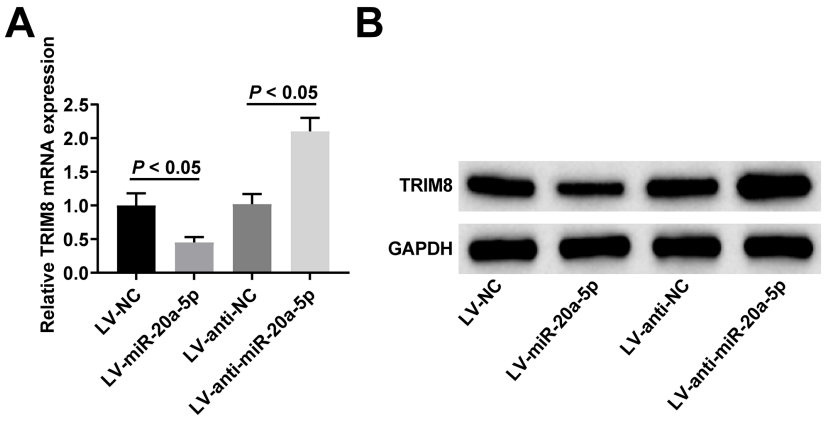

Fig. S3 miR-20a-5p inhibiting TRIM8 expression. A/B: RT-qPCR and Western blot analysis to detect TRIM8 expression. Values are expressed as mean ± SD. Comparisons between two groups were made using independent samples *t*-test while comparisons between multiple groups used one-way ANOVA and Tukey's post hoc test.